Flame synthesis of calcium carbonate nanoparticles

Matthias Huber,[a] Wendelin J. Stark,*[a] Stefan Loher,[a] Marek Maciejewski,[a] Frank Krumeich[b] and Alfons Baiker[a]

Received (in Cambridge, UK) 4th August 2004, Accepted 1st November 2004
First published as an Advance Article on the web 13th December 2004
DOI: 10.1039/b411725e

Calcium carbonate nanoparticles of 20–50 nm size were obtained from a flame spray process where combustion of specific calcium-containing precursors results in amorphous or crystalline calcium carbonate particles depending on the spray flow conditions.

Ultrafine calcium carbonate ($CaCO_3$) particles have a variety of applications in paper, rubber and paint manufacturing, cosmetics, as nucleating agents or fillers in polymerization,[1a–e] and have even been suggested for use in drug delivery.[1f] The most prominent aerosol nanoparticles, silica and titania, are used on a megaton scale in pigments, polymers and as powder flowing aids.[2a–c] Making calcium carbonate of similar morphology would allow the replacement of persistent silica or titania by a bio-degradable nanoparticle. Grinding yields densely agglomerated or unagglomerated nanoparticles.[1a,3a] Detailed investigations on precipitation[3a–c] methods included the influence of varying pH[4a,b] and calcium to carbonate ratio on nucleation and growth rate. Sohnel and Mullin[4c] investigated the effect of impurities on morphology and found a significant influence of anions and cations on size and crystal phase. High-gravity reactive precipitation yielded nanoparticles of 17–36 nm in size.[5] In heterogeneous systems, carbonation of a $Ca(OH)_2$ slurry in a three-phase gas–liquid–solid reacting system afforded nanoparticles with a diameter of up to 500 nm which could be decreased to 70 nm by increasing stirring or adding 1 vol.% of terpinol.[4e] Beyond suspensions[3b] or emulsions,[3c] Willert *et al.* synthesized calcium carbonate nanoparticles by miniemulsification of molten salts.[3a] McCormick *et al.*[1a] applied mechanochemical synthesis by placing $CaCl_2$, Na_2CO_3 and NaCl in a ball miller and obtained $CaCO_3$ in a NaCl matrix.

The present methods result in rather dense, agglomerated particles if made in the liquid phase or unagglomerated particles that later form soft agglomerates upon usage. In order to obtain a stable, open and well-agglomerated morphology, a gas-phase process as in the case of silica manufacturing is required. Here, we would like to show that calcium carbonate nanoparticles can be prepared by a direct flame spray process, similar to the silica aerosol process.[2a–c]

Feeding calcium 2-ethylhexanoate precursors[2e] into a methane–oxygen-flame yields calcium carbonate nanoparticles of varying surface structure and crystallinity (Fig. 1, 2). Analysis by X-ray diffraction (XRD) shows that high fuel to oxygen ratios (7/3, Fig. 3) result in irregularly shaped agglomerates of calcium carbonate crystallites and distinct XRD signals.

Using more oxygen and less fuel decreases the mean flame temperature and leads to the formation of amorphous calcium carbonate. The degree of crystallinity was measured by differential scanning calorimetry (DSC). Crystallization can be observed as an exothermic event at around 310 °C (inset Fig. 3). Comparison of XRD patterns before (1) and after (2) heat treatment corroborate an increase of the crystalline calcium carbonate after heat treatment (Fig. 3). Transmission electron microscopy images of calcium carbonate nanoparticles before (Fig. 1) and after sintering (Fig. 2, inset) further confirm the presence of amorphous calcium carbonate nanoparticles for low fuel to oxygen ratios during synthesis. High fuel to oxygen ratio results in well-sintered, highly crystalline nanoparticles (Fig. 2) that resemble corresponding amorphous samples after sintering (Fig. 2, inset). The amorphous calcium carbonate samples were further analyzed by mass spectroscopy (Fig. 4). At low temperature, physisorbed water (m/z = 18) was released from the sample and accounted for 2.6 wt% water. Crystallization of amorphous calcium carbonate at 300 °C was followed by the release of chemically bound water (2.3 wt%) and traces of NO (m/z = 30). The latter suggests the presence of minute amounts of calcium nitrite or nitrate formed during synthesis. An endothermic signal at 750 °C, simultaneous mass loss (TG) and the evolution of carbon dioxide (m/z = 44) prove the decomposition of calcium carbonate to calcium oxide and carbon dioxide. The calcium carbonate content was determined from TG and depends on synthesis conditions (Table 1). Increasing both oxygen and precursor feed but keeping their ratio constant had little effect on the product (note the similar

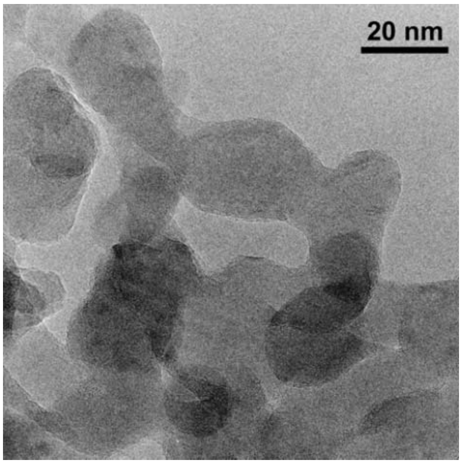

Fig. 1 Transmission electron micrograph of flame-made calcium carbonate nanoparticles resulting from a *low fuel to oxygen ratio*. Particles are mainly amorphous and exhibit a relatively smooth surface. The morphology of the calcium carbonate nanoparticles resembles the structure of fumed silica.

---

*wendelin.stark@chem.ethz.ch

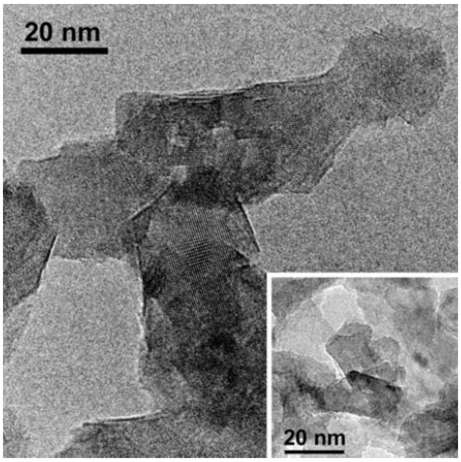

Fig. 2 Crystalline particles with a rough surface and clearly discernible crystallites are obtained at *high fuel to oxygen ratio* during synthesis. Similar particles can be obtained by sintering amorphous calcium carbonate (inset).

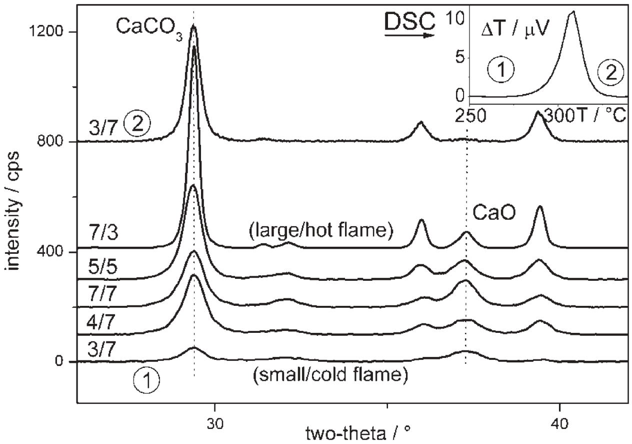

Fig. 3 XRD patterns of calcium carbonate particles produced at different flame conditions. (*x*/*y*) with *x* being ml fuel/min and *y* L oxygen/min (see text).

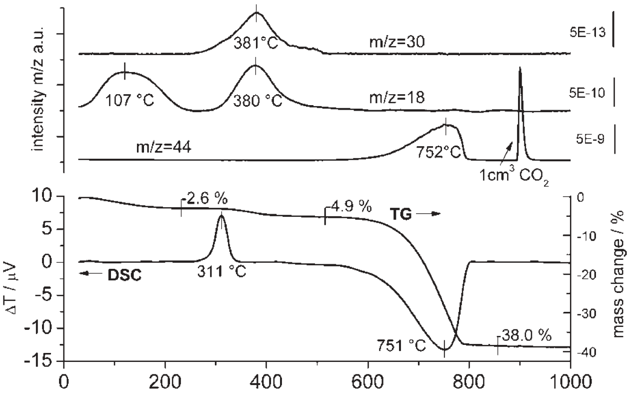

Fig. 4 Thermal analysis and mass spectroscopy of evolving gases of calcium carbonate nanoparticles upon heat treatment. Crystallization of amorphous calcium carbonate occurs at 310 °C and the sample decomposes above 700 °C.

Table 1 Calcium carbonate content of particles prepared by using different flame synthesis parameters

Fuel	Oxygen	CaCO$_3$[a]	BET[b]
7 ml min^{-1}	3 L min^{-1}	90 wt%	31.1 ± 0.8 m^2 g^{-1}
5 ml min^{-1}	7 L min^{-1}	81 wt%	84.5 ± 1.2 m^2 g^{-1}
4 ml min^{-1}	7 L min^{-1}	78 wt%	97.3 ± 2 m^2 g^{-1}
3 ml min^{-1}	7 L min^{-1}	75 wt%	102.6 ± 2 m^2 g^{-1}
7 ml min^{-1}	7 L min^{-1}	67 wt%	59.0 ± 1 m^2 g^{-1}

[a] Calculated from thermal analysis. Error: ± 1 wt%. [b] Measured by nitrogen adsorption at 77 K.

XRD patterns of 5/5 and 7/7 in Fig. 3), suggesting that the aerosol synthesis can be scaled up.

While flame conversion of most metal precursors results in oxides,[2b–d] the basic calcium oxide can be re-carbonized *in situ* during the cool-down in the off-gas of the flame. At high sheer rate (high gas to liquid flow rate in the spray), the cool-down and carbonization are fast and mainly amorphous calcium carbonate is observed. High fuel to oxygen ratio reduces cool down and gives more time for crystallization of the sample (see figures). Consequently, a more sintered product is obtained. The present aerosol method gives access to bio-degradable nanoparticles of a morphology that is likely to have broad industrial applications. Further applications may arise from modifications in compositions and associated new functionality.†

Matthias Huber,[a] Wendelin J. Stark,*[a] Stefan Loher,[a]
Marek Maciejewski,[a] Frank Krumeich[b] and Alfons Baiker[a]
[a]*Institute for Chemical and Bioengineering, ETH Hönggerberg HCI E 107, CH-8093, Zürich, Switzerland.*
E-mail: wendelin.stark@chem.ethz.ch; Fax: +41 1 633 10 83;
Tel: +41 1 633 09 80
[b]*Laboratory of Inorganic Chemistry, ETH Hönggerberg HCI G 105, CH-8093, Zürich, Switzerland*

Notes and references

† Calcium carbonate was prepared by flame spray pyrolysis[2d] using calcium oxide (99.9%, Aldrich) dissolved in equivalent volumes of 2-ethylhexanoic acid (purum., ⩾99%, Fluka)/xylene (96%, Riedel deHaen) as precursors[2e] (concentration 0.4 M). The liquid mixtures were fed through a capillary (diameter 0.4 mm) into a methane/oxygen flame at rates varying from 3 to 7 ml min^{-1}. Oxygen (3 to 7 L min^{-1}, 99.8%, Pan Gas, constant pressure drop at the capillary tip 1.5 bar) was used to disperse the liquid leaving the capillary. A stable combustion was achieved by applying a sheath gas (oxygen, 230 L h^{-1}, 99.8%, Pan Gas) through a concentric sinter metal ring. Calibrated mass flow controllers (Bronkhorst) were used to monitor all gas flows. The as-formed particles were collected on a glass fibre filter (Whatmann GF/A, 25.7 cm in diameter), placed on a cylinder mounted above the flame, with the aid of a vacuum pump (Vaccubrand). For analysis, thermal effects were detected by means of differential scanning calorimetry (DSC) on a Netzsch STA 409 simultaneous thermal analyser equipped with a mass spectrometer. Signals were recorded during heating of the sample in argon with a rate of 10 K min^{-1}. X-ray diffraction was conducted on a Siemens powder X-ray diffractometer using Ni-filtered CuK$_\alpha$ radiation in step mode with a step size of 0.01° and 0.3 s. TEM images were recorded on a CM30 ST (Philips, LaB$_6$ cathode, operated at 300 kV, point resolution ~ 4 Å). Particles were deposited onto a carbon foil supported by a copper grid.

1 (*a*) P. G. McCormick and T. Tsuzuki, *Metastable Mech. Alloyed Nanocryst. Mater.*, 2002, **386–3**, 377; (*b*) M. Vucak, M. N. Pons, J. Peric and H. Vivier, *Powder Technol.*, 1998, **97**, 1, 1; (*c*) N. Cheng, C. Wan and Y. Zhang, *Polym. Test.*, 2004, **23**, 169; (*d*) C.-M. Chan, J. Wu, J.-X. Li and Y.-K. Cheung, *Polymer*, 2002, **43**, 10, 2981; (*e*) M. L. Di Lorenzo, M. E. Errico and M. Avella, *J. Mater. Sci.*, 2002,

37, 11, 2351; (*f*) J. F. Chen, H. M. Ding, J.-X. Wang and L. Shao, *Biomaterials*, 2004, **25**, 4, 723.

2 (*a*) S. E. Pratsinis, *Prog. Energy Combust. Sci.*, 1998, **24**, 3, 197; (*b*) C. R. Bickmore, K. F. Waldner, R. Baranwal, D. R. Treadwell, R. Narayanan and R. M. Laine, *J. Am. Ceram. Soc.*, 1998, **81**, 1477; (*c*) W. J. Stark and S. E. Pratsinis, *Powder Technol.*, 2002, **126**, 2, 103; (*d*) L. Mädler, H. K. Kammler, R. Mueller and S. E. Pratsinis, *J. Aerosol Sci.*, 2002, **33**, 2, 369; (*e*) W. J. Stark, L. Mädler and S. E. Pratsinis, *WO2004/005184*, 2004.

3 (*a*) M. Willert, R. Rothe, K. Landfester and M. Antonietti, *Chem. Mater.*, 2001, **13**, 12, 4681; (*b*) S. Minayoshi, N. Saito, M. Hanazaki, H. Nishioka, S. Kuroda, M. Takahashi, S. Shimizu and N. Maida, *EP459399*, 1991; (*c*) J. D. Hopwood and S. Mann, *Chem. Mater.*, 1997, **9**, 8, 1819.

4 (*a*) J. Gomez-Morales, J. Torrent-Burgues, A. Lopez-Macipe and R. Rodriguez-Clemente, *J. Cryst. Growth*, 1996, **166**, 1–4, 1020; (*b*) J. Gomez-Morales, J. Torrent-Burgues and R. Rodriguez-Clemente, *J. Cryst. Growth*, 1996, **169**, 2, 331; (*c*) O. Sohnel and J. W. Mullin, *J. Cryst. Growth*, 1982, **60**, 2, 239; (*d*) L. Xiang, Y. Xiang, Y. Wen and F. Wei, *Mater. Lett.*, 2004, **58**, 6, 959.

5 J. F. Chen, Y. Wang, F. Guo, X. Wang and C. Zheng, *Ind. Eng. Chem. Res.*, 2000, **39**, 3, 948.